J Physiol 587.10 (2009) pp 2299–2312

The Journal of Physiology

Rapid Ca^{2+} flux through the transverse tubular membrane, activated by individual action potentials in mammalian skeletal muscle

Bradley S. Launikonis[1,2], D. George Stephenson[3] and Oliver Friedrich[1]

[1] *School of Biomedical Sciences, University of Queensland, Brisbane, Queensland, Australia*
[2] *Section of Cellular Signaling, Department of Molecular Biophysics and Physiology, Rush University Medical Center, Chicago, IL, USA*
[3] *Department of Zoology, La Trobe University, Melbourne, Victoria, Australia*

Periods of low frequency stimulation are known to increase the net Ca^{2+} uptake in skeletal muscle but the mechanism responsible for this Ca^{2+} entry is not known. In this study a novel high-resolution fluorescence microscopy approach allowed the detection of an action potential-induced Ca^{2+} flux across the tubular (t-) system of rat extensor digitorum longus muscle fibres that appears to be responsible for the net uptake of Ca^{2+} in working muscle. Action potentials were triggered in the t-system of mechanically skinned fibres from rat by brief field stimulation and t-system $[Ca^{2+}]$ ($[Ca^{2+}]_{t\text{-}sys}$) and cytoplasmic $[Ca^{2+}]$ ($[Ca^{2+}]_{cyto}$) were simultaneously resolved on a confocal microscope. When initial $[Ca^{2+}]_{t\text{-}sys}$ was $\geq$ 0.2 mM a Ca^{2+} flux from t-system to the cytoplasm was observed following a single action potential. The action potential-induced Ca^{2+} flux and associated t-system Ca^{2+} permeability decayed exponentially and displayed inactivation characteristics such that further Ca^{2+} entry across the t-system could not be observed after 2–3 action potentials at 10 Hz stimulation rate. When $[Ca^{2+}]_{t\text{-}sys}$ was closer to 0.1 mM, a transient rise in $[Ca^{2+}]_{t\text{-}sys}$ was observed almost concurrently with the increase in $[Ca^{2+}]_{cyto}$ following the action potential. The change in direction of Ca^{2+} flux was consistent with changes in the direction of the driving force for Ca^{2+}. This is the first demonstration of a rapid t-system Ca^{2+} flux associated with a single action potential in mammalian skeletal muscle. The properties of this channel are inconsistent with a flux through the L-type Ca^{2+} channel suggesting that an as yet unidentified t-system protein is conducting this current. This action potential-activated Ca^{2+} flux provides an explanation for the previously described Ca^{2+} entry and accumulation observed with prolonged, intermittent muscle activity.

(Received 6 January 2009; accepted after revision 25 March 2009; first published online 30 March 2009)
Corresponding author B. S. Launikonis: School of Biomedical Sciences, University of Queensland, Brisbane, Qld 4072, Australia. Email: b.launikonis@uq.edu.au
Website: http://profiles.bacs.uq.edu.au/Bradley.Launikonis.html

Ca^{2+} entry into cells is a fundamental process to regulate cytoplasmic $[Ca^{2+}]$, $[Ca^{2+}]$ in intracellular stores and many Ca^{2+}-dependent intracellular processes from gene expression to muscle contraction (Berchtold *et al.* 2000). Cardiac cells have an absolute requirement for Ca^{2+} entry via the L-type Ca^{2+} channel upon excitation to induce Ca^{2+} release from the sarcoplasmic reticulum (SR) and consequently activate the contractile apparatus. Another isoform of the L-type Ca^{2+} channel also exists in skeletal muscle (α_{1s} of the dihydropyridine receptor (DHPR)) but the duration of membrane depolarization during a single action potential in skeletal fibres is too brief (2–5 ms), compared to that in cardiomyocytes (100–250 ms), to activate this channel to any detectable degree. Instead, the α_{1s}-subunit of the L-type Ca^{2+} channel in skeletal muscle acts as a voltage sensor, which directly activates Ca^{2+} release from the SR (Melzer *et al.* 1995). This is not to say that skeletal muscle L-type Ca^{2+} channels cannot pass Ca^{2+}, they simply require a relatively long period of depolarization that does not occur under normal physiological conditions, i.e. during a single twitch or during brief tetani. Yet, there is evidence for Ca^{2+} entry associated with periods of low frequency excitation (1–2 Hz) of skeletal muscle (Bianchi & Shanes, 1959; Curtis, 1966; Gissel & Clausen, 1999), but the mechanism of Ca^{2+} entry during normal excitation in adult skeletal muscle fibres has not been identified due to inherent limitations in the techniques used to record very small Ca^{2+} fluxes.

DOI: 10.1113/jphysiol.2009.168682

There are major limitations upon recording very small Ca^{2+} fluxes with conventional electrophysiological techniques. In the whole-cell configuration of skeletal muscle fibres resolution of the minute currents in the lower picoamp range are usually prevented by noise levels determined by the use of feedback resistors (50–500 MΩ) to resolve currents between 0.1 and 200 nA (e.g. MultiClamp Commander specifications, Molecular Devices, USA). The problem of recording small Ca^{2+} currents is further compounded by the long depolarizing pulses that significantly reduce the driving force for Ca^{2+} (DF_{Ca}) entry. Classically these small currents would be assessed with patch-clamp techniques. However, in skeletal muscle the major interface between myoplasm and extracellular environment is the transverse tubular system (t-system) membrane which exists as deep invagination from the surface membrane (Peachey, 1966). This membrane is not accessible to microelectrodes. A more sensitive technique employs mechanically skinned fibres in conjunction with a low affinity Ca^{2+}-sensitive dye trapped in the t-system, the source compartment for the Ca^{2+} influx. The use of this preparation allows the derivation of t-system Ca^{2+} fluxes from net changes in t-system $[Ca^{2+}]$ ($[Ca^{2+}]_{t\text{-}sys}$). This method has enabled real-time analysis of the store-operated Ca^{2+} current across the t-system in muscle during Ca^{2+} release (Launikonis *et al.* 2003; Launikonis & Ríos, 2007) which has been inaccessible to careful electrophysiological measurements (Allard *et al.* 2006).

In the present study we simultaneously recorded dynamic changes in $[Ca^{2+}]$ in the sealed t-system ($[Ca^{2+}]_{t\text{-}sys}$) using the sensitive 'shifted excitation and emission ratioing' (SEER) $[Ca^{2+}]$ imaging technique (Launikonis *et al.* 2005) and changes in cytoplasmic $[Ca^{2+}]$ in response to single action potentials (Posterino *et al.* 2000) under conditions approaching the normal distribution of the major physiologically occurring ions. This allowed us to directly describe, for the first time, the t-system action potential-activated Ca^{2+} current (APACC) and characterize its basic properties.

Methods

All experimental methods were approved by the Institutional Animal Care and Use Committee at Rush University. Ten Sprague–Dawley rats (250–300 g) were used in this study. Rats were killed by a rising concentration of CO_2 and the extensor digitorum longus (EDL) muscles were rapidly excised. Muscles were then placed in a Petri dish under paraffin oil above a layer of Sylgard.

The method of trapping fluorescent dye in the sealed t-system has been described (Lamb *et al.* 1995). Briefly, small bundles of fibres were isolated and exposed to a 'dye solution' while still intact. Individual fibres were then isolated and mechanically skinned. Skinned fibres were transferred to a custom-built experimental chamber with a coverslip bottom, where they were bathed in a standard K^+-repriming solution. The preparation was positioned in the chamber between two platinum electrodes, which ran parallel to the longitudinal axis of the mounted fibre. Skinned fibres were electrically stimulated with a field pulse at approximately 70 V cm^{-1} for 2 ms, as described previously (Posterino *et al.* 2000; Launikonis *et al.* 2006).

Solutions

The dye solution was a physiological solution containing (mM): NaCl, 145; KCl, 3; $CaCl_2$, 2.5; $MgCl_2$, 2; mag-indo-1 salt, 10; and Hepes; 10 (pH adjusted to 7.4 with NaOH). Note that the apparent [mag-indo-1] per pixel in the confocal image associated with the t-system was in the range 2–50 μM. Given the much smaller volume of the t-system compared with the pixel size, the true [mag-indo-1] value in the t-system must be much higher than 50 μM but will be still considerably lower than the 10 mM applied to the external environment of the intact fibres. This is because there is dye loss from the t-system during the skinning procedure and some dye is also removed from the sealed t-system by anion transporters (Launikonis & Stephenson, 2002). The standard K^+-repriming solution contained (mM): K^+, 126; Na^+, 36, Mg^{2+}, 1; HDTA, 50; Hepes, 90; EGTA, 0.01; ATP, 8; creatine phosphate, 10; and rhod-2, 0.1. Osmolality was adjusted to 290 ± 10 mosmol kg^{-1} with sucrose and pH was set to 7.1 with KOH. This solution kept the sealed t-system polarized (Lamb & Stephenson, 1994). *n*-Benzyl-*p*-toluene sulphonamide (BTS; 50 μM; Sigma-Aldrich Co., St Louis, MO, USA) was added to suppress contraction without affecting excitability or Ca^{2+} movements (Cheung *et al.* 2002; Macdonald *et al.* 2005). 2-Aminoethyl diphenyl borate (2-APB; 0.1 mM; Sigma-Aldrich) and SKF-96356 (25 μM; Sigma-Aldrich) were added to solutions as required from a 100 mM stock in DMSO.

Confocal imaging and analysis

Imaging was as described in Launikonis *et al.* (2005) using a TCS SP2 confocal system (Leica) in the laboratory of Eduardo Ríos (Rush University Medical Center, Chicago, USA). Line scan images were obtained at 0.625 ms line^{-1} and 0.23 μm pixel^{-1}, for a group scanning speed of 1.875 ms line^{-1}. Simultaneous monitoring of $[Ca^{2+}]_{t\text{-}sys}$ and cytoplasmic dye required three interleaved images: $F_1(x, t)$, $F_2(x, t)$ and $F_3(x, t)$, with excitation lines at 351, 364 and 543 nm and emission bands of 390–440, 465–535 and 562–666 nm, respectively. SEER ratio images $R(x, t) = F_1(x, t)/F_2(x, t)$ were used to derive $[Ca^{2+}]_{t\text{-}sys}$ as

described in Launikonis & Ríos (2007) using the equation:

$$[Ca^{2+}](x, t) = \gamma K_D[R(x, t) - R_{min}]/[R_{max} - R(x, t)], \quad (1)$$

where γK_D, R_{max} and R_{min} were 0.615 mM, 4.82 and 0.45, respectively. These parameters were determined *in situ* as described by Launikonis & Ríos (2007). $F_3(x, t)$ of rhod-2 in the internal solution was normalized by dividing it by the average resting value $F_{3,0}$, a common procedure when using a non-ratiometric indicator of $[Ca^{2+}]_{cyto}$.

SEER images of 50 μM indo-5F in the cytoplasmic solution were also recorded during field stimulation. The parameters to define $[Ca^{2+}]_{cyto}$ from R in the cytoplasm were derived *in situ* and the following parameters were derived from equations defined in Launikonis *et al.* (2005): $R_{min} = 0.5$; $R_{max} = 3.2$; and $\gamma K_D = 2.38$ μM.

Results

Action potential-induced Ca^{2+} release in mechanically skinned fibres

Figure 1 shows the transient rise in cytoplasmic $[Ca^{2+}]$ ($[Ca^{2+}]_{cyto}$) in a mechanically skinned fibre from the EDL muscle of the rat in response to electrical field stimulation. The ratio ($R = F_1/F_2$) image of indo-5F fluorescence in the cytoplasm is displayed in panel *A* and the simultaneous rhod-2 fluorescence image (F_3) in *B*. The spatially averaged signals are represented in *C* showing little difference between the time course of the R and F_3 signals. Note also that there was a spatially and temporally homogeneous rise in the fluorescence signals upon field stimulation. In the absence of the sarcolemma this indicates that an action potential was triggered in each transverse tubule in the imaging plane, which then synchronously propagated radially across the fibre.

The rise time of the fluorescence signals was 5.6 and 7.5 ms for F_3 and R, respectively, and the peak of $[Ca^{2+}]_{cyto}$ that is not corrected for the delay with which R tracks the actual $[Ca^{2+}]_{cyto}$ changes, was 1.1 μM (Fig. 1*C*). This is similar to recordings made in intact skeletal muscle fibres using similar dyes (Westerblad & Allen, 1996; Jacquemond, 1997; Baylor & Hollingworth, 2003).

Correcting for the delay with which R tracks the actual $[Ca^{2+}]_{cyto}$ (Fig. 1*C*) using eqn (2) from Bakker *et al.* (1997):

$$[Ca^{2+}]_C = [Ca^{2+}]_R + (d[Ca^{2+}]_R/dt) \times (k_{-1}(1 + [Ca^{2+}]_R/\gamma K_D))^{-1}$$

where k_{-1} for indo-5F was assumed to be 75 s^{-1} and γK_D is 2.38 μM. $[Ca^{2+}]_R$ is $[Ca^{2+}]_{cyto}$ directly calculated from R of indo-5F in cytoplasm. Because k_{+1} is approximately the same for indo-1 and indo-5F, the k_{-1} of indo-5F will increase by the ratio of the K_D values of indo-5F/indo-1. Zhou *et al.* (2006) calculated γK_D of indo-1 in the cytoplasm to be 1.62 μM. Thus a k_{-1} of 55 s^{-1} for indo-1 (Westerblad & Allen, 1996) equates to 75 s^{-1} for indo-5F. The inset in Fig. 1*A* shows that the actual $[Ca^{2+}]_{cyto}$ transient is much faster than the corresponding fluorescence signals (R, F_3) and reaches a $[Ca^{2+}]$ peak of 4 μM that is markedly greater than the apparent $[Ca^{2+}]$ of 1.1 μM if the correction was not applied (see also Baylor & Hollingworth, 1988). However, the peak of the Ca^{2+} transient is also most likely 'blunted' by the (low) temporal resolution of the group scanning speed of the three lasers (2 ms; Royer *et al.* 2008).

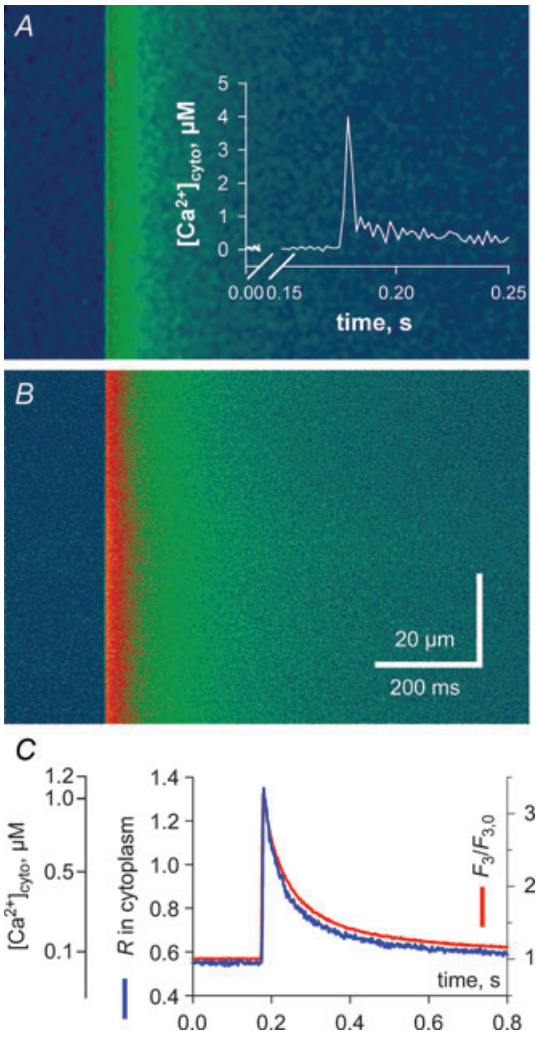

Figure 1. Action potential activation of a global Ca^{2+} transient in a skinned fibre
A, ratio (R) in the cytoplasm derived from the indo-5F fluorescence, which was simultaneously recorded with the F_3 image of rhod-2 fluorescence in the cytoplasm (*B*) during a twitch in a skinned fibre from rat EDL muscle. *C*, spatially averaged profiles of R and F_3. Inset in *A* is the derived Ca^{2+} transient from R corrected for dye kinetics, as described in the text.

Thus the skinned fibre releases Ca^{2+} at a normal rate and magnitude during excitation–contraction (EC) coupling (Posterino & Lamb, 2003; Launikonis *et al.* 2006). Indeed the absence of the sarcolemma in skinned fibres, like the absence of a nerve supply in isolated intact fibres, makes little difference to the function of the EC coupling machinery within the triads. Therefore we used this preparation to determine whether there is a Ca^{2+} current across the t-system associated with an action potential using a recently developed fluorescence technique (Launikonis & Ríos, 2007).

A rapidly available pathway for Ca^{2+} movement across the t-system

In these experiments, the ratiometric Ca^{2+}-sensitive fluorescent dye mag-indo-1 was trapped in the sealed t-system to allow the measurement of its $[Ca^{2+}]$, $[Ca^{2+}]_{t\text{-}sys}$. Rhod-2 was simultaneously present in the cytoplasmic environment to allow myoplasmic $[Ca^{2+}]$ measurements, $[Ca^{2+}]_{cyto}$. Note that $[Ca^{2+}]_{t\text{-}sys}$ in skinned fibres can be easily altered over a wide range of concentrations in the same preparation by altering the level of t-system membrane polarization and $[Ca^{2+}]_{cyto}$ (Launikonis & Ríos, 2007). In order to help maximally polarize the t-system of skinned fibre preparations and fully re-prime the voltage sensors, a Cl^--free internal bathing solution was used (see Posterino *et al.* 2000; Methods). Note, however, that when the t-system is hyperpolarized, the ability of the t-system Ca^{2+} pumps to maintain a large $[Ca^{2+}]_{t\text{-}sys}$ is reduced and the absence of Cl^- will limit the rate at which the t-system can sustain trains of action potentials (Dutka *et al.* 2008). The maximum stimulation rate used in this study was 10 Hz.

Figure 2 illustrates experiments comparing the evolution of $[Ca^{2+}]_{t\text{-}sys}$ starting from two different levels (panels *A* or *B*). The action potential-induced Ca^{2+} release from the SR is visualized in panels *Aa* and *Ba* by corresponding changes in confocal line scans of rhod-2 fluorescence intensity (F_3), while the changes in the mag-indo-1 ratio images $R(x, t)$, reflecting changes in $[Ca^{2+}]_{t\text{-}sys}$, are shown in panels *Ab* and *Bb*. The spatially averaged values from these images are plotted *vs.* time in the respective *c* panels in Fig. 2. From Fig. 2*A*, one can observe a decrease in the t-system *R* value right from the time when the peak of the cytoplasmic $[Ca^{2+}]$ was reached. This indicates that there was a net flow of Ca^{2+} from the t-system into the cytoplasm following an action potential. In contrast, when the $[Ca^{2+}]_{t\text{-}sys}$ was low at the time an action potential was triggered (Fig. 2*B*), there was a net initial outward flow of Ca^{2+} from the cytoplasm into the t-system that was rapidly reversed during the remainder of the action potential duration.

Because the t-system volume does not change during release (Launikonis & Ríos, 2007) the flux of Ca^{2+} across the t-system membrane is equal to $\beta \times d[Ca^{2+}]_{t\text{-}sys}/dt$, where β is a proportionality constant, representing the t-system Ca^{2+}-buffering capacity (Launikonis & Ríos, 2007). In Fig. 2*Ad*, $d[Ca^{2+}]_{t\text{-}sys}/dt$ has been derived from an exponential fit to the $[Ca^{2+}]_{t\text{-}sys}$ data in panel *Ac* (as derived from measured *R* values, eqn (1), Methods). Derivatives were calculated from fitted curves to the raw data in Fig. 2*Ac* to reduce the otherwise large amount of noise. The calculated changes in the membrane potential, V_m, during an action potential are also shown in panel *Ad*. The action potential was reconstructed as the sum of two first-order exponential functions, one rising with rate constant of $0.4\ ms^{-1}$ and the other decaying with a rate constant of $0.23\ ms^{-1}$ (Friedrich *et al.* 2004). The peak of the action potential and Ca^{2+} transient were assumed to be within 3 ms of each other, in line with experimental data (Delbono & Stefani, 1993; Claflin *et al.* 1994) and the argument made below. The action potential had a duration of < 6 ms (Nielsen *et al.* 2004; Friedrich *et al.* 2004) with a reduced peak at +10 mV because $[Na^+]_{cyto}$ was 36 mM (Cairns *et al.* 2003) in the internal solution. In the example shown in Fig. 2*A*, the exponentially decaying Ca^{2+} flux was activated within milliseconds of the peak of the action potential-induced cytoplasmic Ca^{2+} transient and then decayed in an exponential manner within 200 ms.

In Fig. 2*Bd*, $d[Ca^{2+}]_{t\text{-}sys}/dt$ has been calculated from $[Ca^{2+}]_{t\text{-}sys}$ in *Bc* and the time course of the action potential is also shown. In this case, there is a clear and rapid flow of Ca^{2+} from the cytoplasmic space to the t-system at the time of excitation followed by a reversed flow within 10–20 ms of smaller magnitude. The rising baseline for *R* in the t-system before stimulation is probably due to gradual Ca^{2+} entry into the t-system mediated by the plasmalemmal Ca^{2+}-ATPase located in the t-system membrane (Sachetto *et al.* 1996) after the t-system Ca^{2+} was initially depleted to very low values (Launikonis *et al.* 2003; Launikonis & Ríos, 2007). Since the Ca^{2+} pump in the t-system continues to transport Ca^{2+} into the t-system for some time over the period shown in panel *Bc*, the absence of a net rise in $[Ca^{2+}]_{t\text{-}sys}$ after the action potential indicates a flow of Ca^{2+} from the t-system into the myoplasm via the pathway initiated by the action potential. This can be quantitatively corrected for as shown in Fig. 3.

The rising baseline due to Ca^{2+} transport into the t-system prior to action potential-induced Ca^{2+} release has been fitted with an exponential and extrapolated for the duration of the measurement (dashed black line in Fig. 3*A*) to the data in Fig. 2*Bc*. The dashed red line in Fig. 3*A* fits the decline of the $[Ca^{2+}]_{t\text{-}sys}$ transient following membrane repolarization, which causes reversal of the DF_{Ca} making the Ca^{2+} flux inward and the dashed green line represents

the decline of the APACC contribution to the Ca^{2+} transient in the t-system, after subtracting the baseline.

Finally, in Fig. 3*B* is shown $d[Ca^{2+}]_{t-sys}/dt$ of the APACC contribution to the Ca^{2+} transient in the t-system which is representative of the APACC itself. The outward Ca^{2+} flux (directed into the t-system) appears slightly longer than predicted by the model of DF_{Ca} (Fig. 2) due to smoothing of the raw data and the temporal resolution of 2 ms but still within experimental errors. This is followed by an inward Ca^{2+} flux which decays exponentially over 100 ms with a rate constant of 24 s^{-1}.

As shown in Fig. 2*Ad*, the APACC in that case could also be fitted with a single exponential for 100 ms or so during the time when the membrane potential must have returned to the resting level. This indicates that once activated, the channels deactivated/inactivated with a rate constant of $25.2 \pm 3.6\ s^{-1}$ ($n = 8$), consistent with the corrected rate of the inward APACC in Fig. 3*A*. Therefore, most of the

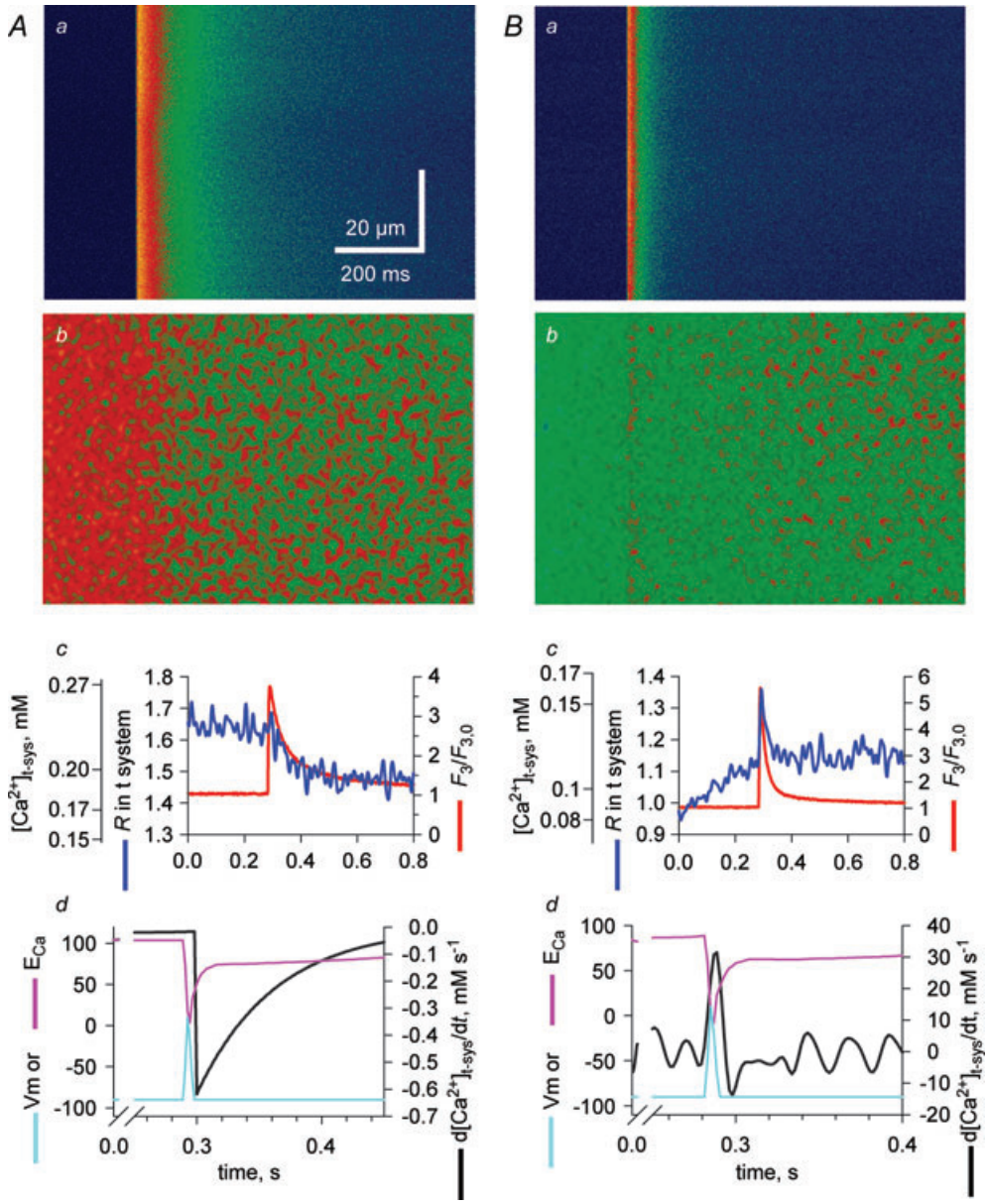

Figure 2. Action potential activation of a t-system Ca^{2+} current
A and *B* represent two examples of simultaneous recordings of *R* in t-system (*b*) and F_3 fluorescence in cytoplasm (*a*) during a field-stimulated action potential. Spatially averaged signals are represented in *c* for each example. Panels *d* represent the Ca^{2+} flux across the t-system, the modelled action potential and E_{Ca}. Note that the line scan images have been digitally filtered and thus the striated pattern of the t-system is no longer apparent (see Supplemental Fig. 1, available online only).

Ca^{2+} flux across the t-system would occur when V_m is close to the resting level.

The peak tubular Ca^{2+} flux initiated by stimulation, peak $-d[Ca^{2+}]_{t\text{-}sys}/dt$, is summarized in Fig. 4 as a function of initial $[Ca^{2+}]_{t\text{-}sys}$. Above 0.2 mM $[Ca^{2+}]_{t\text{-}sys}$, flux was inward (indicating net loss from the t-system) and clearly depended on the Ca^{2+} gradient in a roughly linear fashion. Below ~0.15 mM $[Ca^{2+}]_{t\text{-}sys}$, peak flux was outward (from cytosol to t-system) although the flux always reversed following repolarization of the t-system.

From Fig. 4 one can see that there is a change in the direction of Ca^{2+} flux across the t-system and therefore, a change in the direction of the driving force for Ca^{2+}, the electrochemical potential difference V_{Ca}, when $[Ca^{2+}]_{t\text{-}sys}$ is about 0.15 mM (the peak becomes outwardly directed, an efflux). Let V_m represent the membrane potential, E_{Ca} the equilibrium potential for Ca^{2+} and $[Ca^{2+}]_{cleft}$ the $[Ca^{2+}]$ on the cytoplasmic side of the t-system wall; then it is possible to calculate V_{Ca} as:

$$V_{Ca} = V_m - E_{Ca} = V_m - (RT/2F) \times \ln([Ca^{2+}]_{t\text{-}sys}/[Ca^{2+}]_{cleft})$$

Hence it is possible to estimate the $[Ca^{2+}]$ peak in the cleft during excitation as greater than the value that annuls V_{Ca}. Thus, if the Ca^{2+} entry pathway was activated and if the inversion occurred at the peak of the action potential or slightly thereafter, when $V_m \sim +10$ mV to -10 mV, $[Ca^{2+}]_{cleft}$ at that time would be $[Ca^{2+}]_{t\text{-}sys} \exp(-2FV_m/RT) = 68\ \mu M$ (at $+10$ mV) to $330\ \mu M$ (at -10 mV). During the time that the flux is outward, the concentration in the cleft should be greater than 68 μM.

Conversely, one can place an upper limit on how late this Ca^{2+} pathway can be activated following an action potential by considering that $[Ca^{2+}]_{cleft}$ following excitation cannot be greater than the $[Ca^{2+}]$ in the SR, which is around 1 mM (Fryer & Stephenson, 1996). Thus, assuming 1 mM as the highest possible $[Ca^{2+}]_{cleft}$ and $[Ca^{2+}]_{t\text{-}sys} = 0.15$ mM, reversal of direction of flux across the t-system membrane would occur at V_m values more positive than -24 mV. This condition would be satisfied only for about 3 ms after an action potential is initiated in the t-system (Woods *et al.* 2004, DiFranco *et al.* 2005). This clearly shows that the action potential-induced Ca^{2+} flux (APACC) is activated very rapidly during an action potential, suggesting that it is mediated by voltage-activated channels.

We have also attempted to block the APACC with pharmacological agents. The non-specific cation channel blocker 2-APB (100 μM), which is commonly used to block transient receptor potential (TRP) channels caused rapid reduction of action potential-induced Ca^{2+} release which was abolished within 2–3 pulses (1–2 min) in three preparations tested (not shown). The current continued to be seen when the responses declined, but given the short time in the presence of 2-APB, it was difficult to assess whether 2-APB had time to equilibrate and bind to t-system membrane proteins, as we have previously

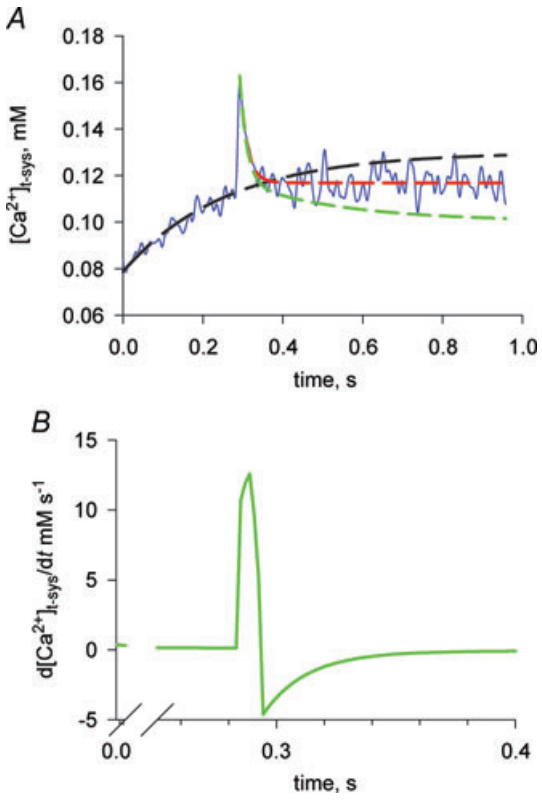

Figure 3. Correction for Ca^{2+} transport into the t-system to observe action potential-activated Ca^{2+} flux at low $[Ca^{2+}]_{t\text{-}sys}$
A, the net change in $[Ca^{2+}]_{t\text{-}sys}$ (from Fig. 2*Bc*) is shown (blue line); an exponential has been fitted to the rising baseline and extrapolated beyond the point where the fibre was stimulated (dashed black line; $k = 3.9 \pm 1.0\ s^{-1}$ and $r^2 = 0.84$); a decaying exponential has been fitted to the net change in $[Ca^{2+}]_{t\text{-}sys}$ from the point where Ca^{2+} flux has become inward (dashed red line; $k = 55.0 \pm 5.0\ s^{-1}$ and $r^2 = 0.54$); and this has been corrected for Ca^{2+} transport (dashed green line; $k = 22.0 \pm 0.7\ s^{-1}$ and $r^2 = 0.92$). *B*, the derivative indicating the Ca^{2+} flux taking into account the correction to remove the influence of Ca^{2+} transport on net $[Ca^{2+}]_{t\text{-}sys}$ measurements is shown. Note the flux is initially outward and then reverses rapidly and continues for some 100 ms.

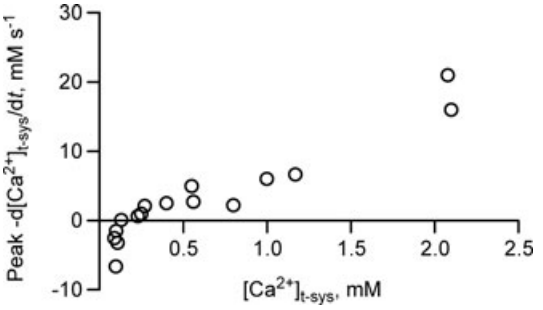

Figure 4. Peak flux of Ca^{2+} across the t-system following an action potential
The peak Ca^{2+} flux at $[Ca^{2+}]_{t\text{-}sys}$ is shown. Result is from 10 fibres.

reported that 2-APB also binds with some delay to the ryanodine receptor RyR1 (Launikonis & Ríos, 2007). Another non-specific cation channel blocker, the drug SKF-96356 (25 μM), which is also used to block TRP channels, caused an immediate block (within seconds) of action potential-induced Ca^{2+} release in the three fibres examined and no APACC current could be observed. Since the drug was shown not to affect the action potentials in cardiac cells (Ju *et al.* 2007), the most likely explanation of our result is that SKF-96356 blocks the APACC without affecting the action potentials. In such a case, the complete and rapid abolition of APACC in the presence of SKF-96356 may suggest that the APACC occurs via TRP channels, although one should bear in mind that SKF-96356 is known to have pleiotropic cellular effects (Leung & Kwan, 1999). Note that the TRP channels that are voltage insensitive (TRPC1/TRPC4, Vandebrouck *et al.* 2002) are excluded as potential candidates. Also excluded as potential candidates are voltage-sensitive TRP channels that activate on a much slower time scale than APACC (e.g. TRPP3 Shimizu *et al.* 2009 and TRPC5: Obukhov & Nowycky, 2008).

Permeability of the APACC

Under the simplifying constant field assumptions, the flux would be governed by the following flux equation (Hodgkin & Katz, 1949):

$$\text{Net } Ca^{2+} \text{ flux} = P_{Ca}\,([Ca^{2+}]_{t-sys}(-\upsilon/(1-\exp\ \upsilon)) - [Ca^{2+}]_{cleft}\upsilon/(1-\exp -\upsilon)),$$

where P_{Ca} is the permeability for Ca^{2+} and $\upsilon = 2FV_m/RT$, assuming that V_m at rest is close to -90 mV, $\upsilon = -7.1$ and the expression becomes:

$$\text{Net } Ca^{2+} \text{ flux} = 7.1\ P_{Ca}([Ca^{2+}]_{t\text{-}sys} - 0.00083[Ca^{2+}]_{cleft})$$

Further considering that under all our conditions $0.00083[Ca^{2+}]_{cleft} < 0.01[Ca^{2+}]_{t\text{-}sys}$, it follows that for all practical purposes the net Ca^{2+} flux across the t-system membrane into the cytoplasmic environment is directly proportional to $[Ca^{2+}]_{t\text{-}sys}$, thus explaining the overall linear dependence of the Ca^{2+} entry in Fig. 4 on $[Ca^{2+}]_{t\text{-}sys}$.

$$\text{Net } Ca^{2+} \text{ flux} \approx 7\ P_{Ca}[Ca^{2+}]_{t\text{-}sys}$$

By dividing now the time course of the Ca^{2+} flux in Fig. 2*Ad* by $7[Ca^{2+}]_{t\text{-}sys}$ we derive the time course of P_{Ca} which should give an indication of the time course of the channel opening. This relationship is shown in Fig. 5.

Regulation of the APACC

If the decrease in t-system flux is deactivation, then a second action potential would be expected to increase the flux to the initial peak, but if it is inactivation, then there would be little or no increase. Figure 6*A–D* shows examples of multiple action potential-activated releases of Ca^{2+} from the SR and the simultaneous movement of $[Ca^{2+}]_{t\text{-}sys}$ from measurements of F_3 fluorescence and R, respectively. Typical responses, elicited by a train of action potentials at 10 Hz, are shown in Fig. 6*A*. Towards the end of the trace a spontaneous action potential was generated in the t-system, some 0.4 s after the field stimulation-elicited action potentials (note that two fibres of the sixteen imaged in this study showed such Ca^{2+} release in response to spontaneous action potentials). The changes in R indicate a single Ca^{2+} influx event from the t-system into the cytoplasmic environment at the start of the electrical stimulation and a second event of similar magnitude associated with the spontaneous response. Changes in R shown in Fig. 6*B* and *C* suggest that action potentials must be spaced at least a few hundred milliseconds apart to induce an inward Ca^{2+} current. When action potentials were elicited at higher rates (last three responses in *C* and *D*), R decreased markedly only following the first action potential. Note that in *B–D*, the first response was elicited by field stimulation while the subsequent responses were due to spontaneous action potentials (field pulses indicated by vertical black bars in Fig. 6). The presence of a t-system Ca^{2+} current during either spontaneous or field pulse-elicited action potentials indicates that the field pulse itself cannot be the cause of any change in R.

It is possible that the inhibition of APACC at higher stimulation frequencies could be due to the maintained higher $[Ca^{2+}]_{cyto}$ and not stimulation frequency. To test this hypothesis skinned fibres were stimulated by trains of action potentials at different rates for longer than 1 s. Figure 7 plots R and rhod-2 fluorescence from fibres that were field stimulated at 2.5 (*A*), 3 (*B*) and 10 Hz (*C*). Each panel is the average of experiments from 3–5 fibres (shifted in time for coincidence of the first peak of F_3). R was

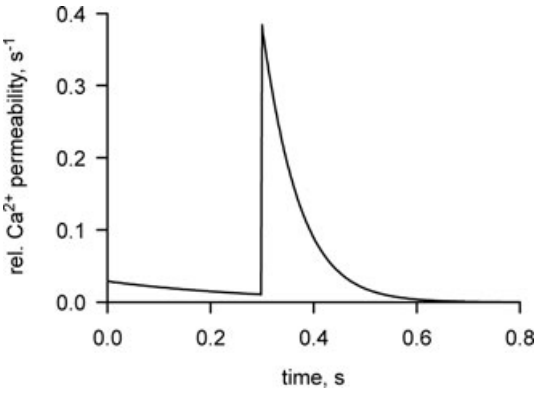

Figure 5. Time course of the permeability to Ca^{2+} across the t-system following an action potential
This relationship has been determined from the flux in Fig. 2*Ad*, as described in the text.

normalized to the initial R (R_0) and corrected for passive leak in each experiment. Minor deviations in stimulation frequency resulted in a small misalignment of some of the peaks of the Ca^{2+} transients, as apparent in the averages shown in *A* and *B*. When the frequency of stimulation was 2.5 or 3 Hz, a drop in R/R_0 (an inward t-system flux) was associated with each twitch (Fig. 7*A* and *B*). A greater drop in R/R_0 was observed following the first two to three action potentials in the 10 Hz train (*C*), indicating a build-up of the effect.

To assess this effect further, the relative t-system Ca^{2+} flux is also plotted in Fig. 7 (green lines). The relationship between relative Ca^{2+} permeability and the time between the first and second action potentials are plotted in Fig. 8. These data are derived from Figs 6 and 7. Specifically the relative t-system Ca^{2+} permeability following the second action potential in a stimulation sequence has been divided by the relative t-system Ca^{2+} permeability following the first action potential and plotted as a function of the time between these action potentials. This analysis clearly shows that the spacing between action potentials affects the relative t-system Ca^{2+} permeability. Only when the stimulation rate is close to 10 Hz is there a marked decline in Ca^{2+} permeability. This indicates that the current

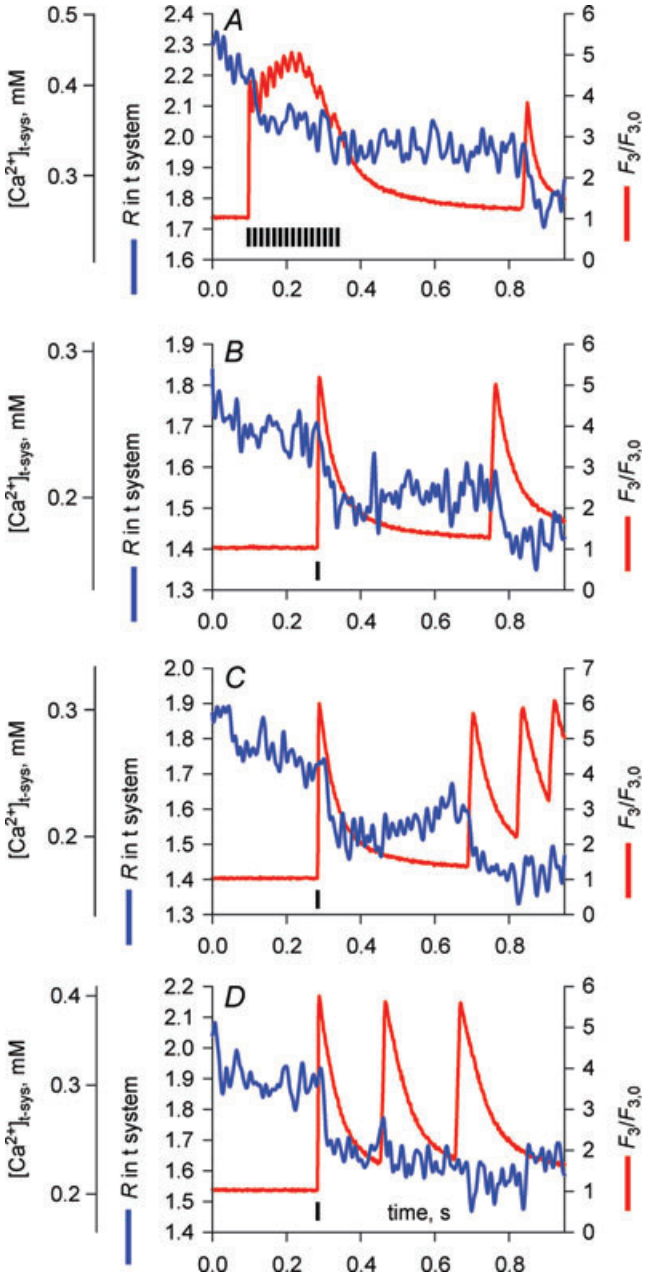

Figure 6. The action potential-activated Ca^{2+} current during different stimulation protocols
A–D, examples of R and F_3 fluorescence during multiple field-stimulated (indicated by black vertical bars) or spontaneous action potentials.

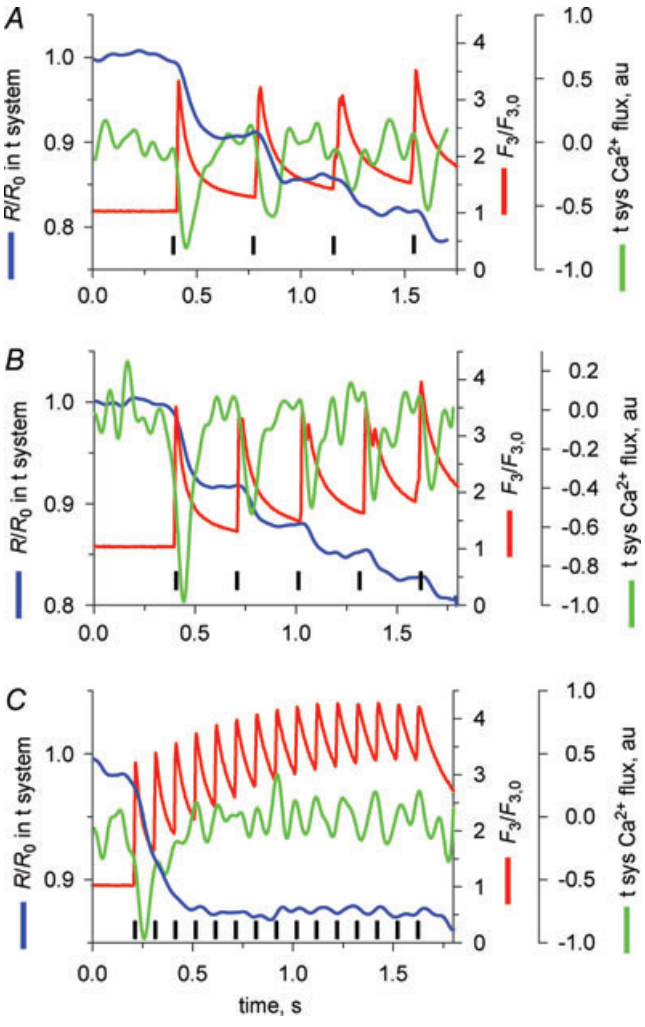

Figure 7. Regulation of the action potential-activated Ca^{2+} current by $[Ca^{2+}]_{cleft}$
Average R and F_3 fluorescence from experiments in 3–5 fibres where preparations were field stimulated (indicated by black vertical bars) at 2.5 (*A*), 3 (*B*) and 10 Hz (*C*). au, arbitrary units.

inactivates rather than deactivates after a single action potential. The continued inhibition of APACC during subsequent action potentials suggests $[Ca^{2+}]_{cyto}$ is keeping the channel in an inactivated state.

Is APACC inactivated by Ca^{2+} flowing from the t-system?

Is the total amount of Ca^{2+} passing through the t-system membrane responsible for inhibiting the channel? In such a case the rate constant of decay of the Ca^{2+} flux would be expected to be greater when the peaks of the Ca^{2+} flux are larger. However, as shown in Fig. 9 this does not appear to be the case ($P = 0.16$). Therefore the bulk $[Ca^{2+}]_{cleft}$, mostly provided by the SR, must be responsible for inactivation of this flux.

Discussion

We show, for the first time, that a Ca^{2+} flux is activated across the t-system of adult mammalian skeletal muscle fibres following a single action potential. A fluorescence method applied in skinned fibres allowed simultaneous imaging of $[Ca^{2+}]_{cyto}$ and $[Ca^{2+}]_{t\text{-}sys}$. SEER imaging (Launikonis *et al.* 2005) of $[Ca^{2+}]_{t\text{-}sys}$ conferred a high sensitivity for observing Ca^{2+} movements across the t-system during excitation and allowed quantification of the t-system flux with millisecond resolution. The flux was found to activate rapidly upon depolarization (~ms) and decay more slowly. The decay was identified as an inactivation, because repeated pulses caused only marginal summation of the flux (Figs 6–8). The properties of this inactivation are consistent with a mechanism mediated by elevated $[Ca^{2+}]$ in the triadic cleft between tubule and terminal cisternae. One consequence of the inactivation is to limit continuous influx of Ca^{2+} during trains of action potentials.

Given fibre diameters of between 40 and 80 μm, peak $-d[Ca^{2+}]_{t\text{-}sys}/dt$ of between 2.5 and 20 mM s^{-1} for most of the tubular Ca^{2+} concentrations (Fig. 4), and assuming a fractional t-system volume of 0.014, the APACC flux translates to a peak Ca^{2+} current of between 8.5×10^{-8} and 2.0×10^{-6} A (cm fibre length)$^{-1}$ when related to the whole fibre volume. Thus, in a silicone-clamp arrangement, as used by Allard *et al.* (2006), with a clamped fibre length of ~200 μm, the expected peak current would be roughly between 2 and 40 nA, depending on the tubular Ca^{2+} concentration. At these intensities, the APACC should be detectable with electrophysiological techniques. However, no action potential-activated Ca^{2+} current was previously reported using electrophysiological techniques.

The apparent discrepancy between our observations and previous electrophysiological measurements may also be explained by differences associated with measurements of Ca^{2+} currents in response to square voltage pulses under voltage-clamp conditions instead of physiological voltage changes associated with an action potential. For example, during a long depolarizing pulse from −80 mV to +20 mV with the voltage-clamp method, the driving force, DF_{Ca} for the Ca^{2+} current initiated by the rapid depolarization will be reduced by more than 5-fold compared to that occurring following the rapid repolarization of an action potential (Fig. 10). The reduced DF_{Ca} would markedly decrease the Ca^{2+} influx under voltage-clamp conditions to a range that may be below the resolution of the macroscopic whole-cell current. It should be stressed that tubular Ca^{2+} currents are not accessible to cell-attached patch-clamp recordings that have a higher resolution due to larger feedback resistors in the headstage and, therefore, completely rely on whole-cell recordings.

It is also possible that APACC can only be revealed following normal excitation in the presence of physiologically occurring monovalent ions Na^+ and K^+, which are not usually present in the experiments with

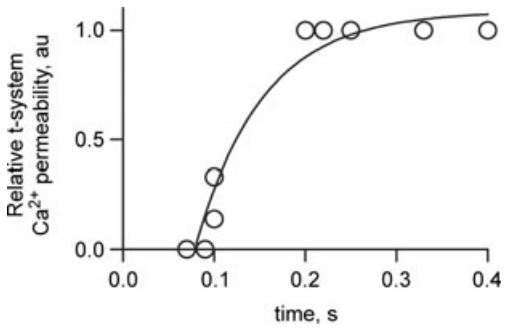

Figure 8. Recovery of APACC from inactivation
From the results in Figs 6 and 7 the relationship between the time between the first and second AP and the relative t-system Ca^{2+} permeability has been plotted. An exponential curve fitted the data ($r^2 = 0.95$, with a rate constant of 13.5 ± 4.5 s^{-1}).

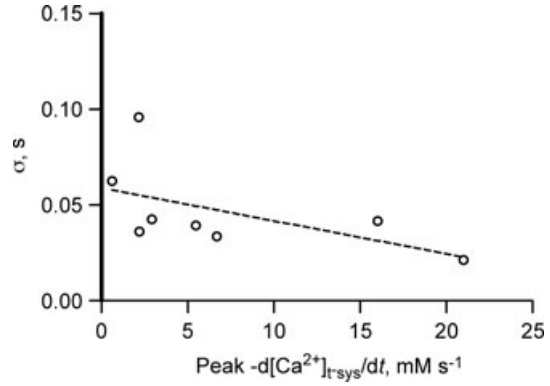

Figure 9. Peak Ca^{2+} flux *vs.* time constant of flux decay
Linear regression through these points is not significant from 0 (null hypothesis accepted, $P = 0.1556$).

conventional electrophysiological techniques mentioned above where background currents have to be blocked by the use of Cs^+, TEA^+ or other organic compounds (Donaldson & Beam, 1983). The typical square pulses applied in voltage-clamp experiments produce a Ca^{2+} transient (or derived release flux) that differs significantly from that produced following physiological excitation. Action potentials produce a Ca^{2+} transient with a rapid rise to a peak that then decays exponentially. This is followed by a peak with every action potential subsequently propagating through the fibre. This Ca^{2+} transient is the same in intact and skinned preparations excited with action potentials (Figs 1, 2, 6 and 7; Baylor & Hollingworth, 1988, 2003; Westerblad & Allen, 1996; Woods *et al.* 2004; Launikonis *et al.* 2006), strongly suggesting the coupling mechanism is exactly the same in intact and skinned fibres. In contrast, voltage-clamped fibres during a square pulse produce a well-described Ca^{2+} transient with a high peak followed by a plateau phase that continues with the depolarizing pulse (e.g. Shirokova *et al.* 1996, 1998). Clearly, the waveform of membrane excitation affects Ca^{2+} release due to the different electrical fields across the DHPR. Thus, functional differences in voltage-sensitive proteins of the t-system are observed when challenged with physiological excitation or long, square pulses. This is a likely reason for APACC not activating under typical voltage-clamp conditions. There is also error in our *in situ* calibration of mag-indo-1 that may have led to an overestimate of the magnitude of APACC (Launikonis *et al.* 2005; Launikonis & Ríos, 2007).

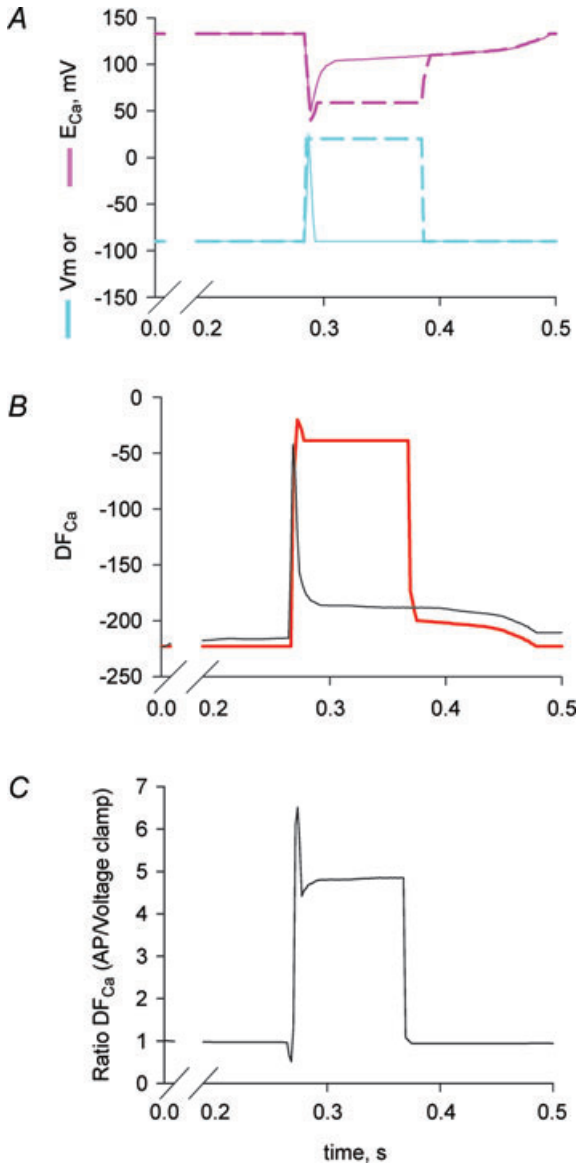

Figure 10. Tubular driving force for Ca^{2+}, DF_{Ca}, is significantly reduced during a voltage-clamp depolarization compared to physiological excitation
A, V_m and E_{Ca} for action potentials (continuous lines) and voltage clamp (dashed lines), calculated as in Fig. 2. *B*, DF_{Ca} during action potential (black line) and voltage clamp (red line). *C*, ratio of DF_{Ca} during an action potential compared to voltage clamp. Note the ratio is close to 5 during stimulation.

Nevertheless, there is supporting evidence for APACC from electrophysiological recordings from intact muscle fibres under current-clamp conditions. For example, the slow depolarization following an action potential during current-clamp conditions of the intact mammalian muscle fibre shown on the pedestal in Fig. 4 of Pedersen *et al.* (2005) and looking like a passive voltage response to the long (25 ms) constant current pulse is consistent with the APACC in terms of magnitude and time course of its inactivation.

Possible sources for APACC

The inactivation of APACC at 10 Hz without noticeable effect on the Ca^{2+} transients (Figs 5 and 6) shows that the flux of Ca^{2+} cannot be passing through t-system channels that are involved in excitation of the membrane, ruling out Na^+ and K^+ channels as pathways of the observed current. Also as T-type channels progressively disappear during maturation within 3 weeks of birth (Beam & Knudson, 1988; Berthier *et al.* 2002), they are unlikely to present a source of Ca^{2+} entry in adult muscle. Furthermore, APACC is clearly activated by voltage, distinguishing it from voltage-independent store-operated Ca^{2+} entry (SOCE; Launikonis & Ríos, 2007).

We do not believe that the Na^+–Ca^{2+} exchanger (NCX) makes a major contribution to the APACC flux under normal conditions because if this were the case, then the APACC flux would be expected to stop and even reverse direction within milliseconds after the t-system membrane repolarizes following an action potential, which was not the case (Fig. 2). Also, in a preceding paper we have shown that the maximal rate of Ca^{2+} uptake by the t-system during SR Ca^{2+} release is around 1 mM s^{-1} (relative to

t-system volume; Launikonis & Ríos, 2007). This uptake must be conducted by the Ca^{2+} pump and NCX. During an action potential, when t-system Ca^{2+} was low (e.g. Fig. 2*B*), we observed Ca^{2+} uptake by the t-system at a rate that was about 5 times greater. This strongly suggests that NCX is not involved in passing this much greater, action potential-induced Ca^{2+} flux.

'Excitation-coupled Ca^{2+} entry' (ECCE) is described as a Ca^{2+} entry pathway in skeletal myotubes that requires retrograde signalling from the ryanodine receptor and continuous (trains of action potentials) or chronic depolarization (Cherednichenko *et al.* 2004). There is no experimental evidence that ECCE is activated by a single action potential, either in myotubes or in adult muscle, distinguishing it from APACC. Indeed it has been recently shown that the majority, if not all, of the ECCE current is carried by the L-type Ca^{2+} channel (Bannister *et al.* 2009). This is consistent with the requirement of ECCE for repetitive or chronic stimulation for activation.

A candidate channel for APACC would be the L-type Ca^{2+} channel. Its voltage–current relationship would suggest activation for most of the potential range covered by a single action potential. However, with its prolonged activation kinetics of more than 40–100 ms time-to-peak in adult fibres (Friedrich *et al.* 1999, 2004) and > 25 ms activation time constants in myotubes (Morrill *et al.* 1998), the L-type Ca^{2+} channel is not fully activated by the brief action potentials in muscle. Importantly, this does not necessarily rule out the DHPR as the protein that conducts APACC during an action potential *per se* because more Ca^{2+} is being carried into the cell upon channel deactivation during repolarization than during the brief depolarization during an action potential. This is mainly a consequence of the much larger DF_{Ca} present during repolarization than depolarization (Fig. 2; Johnson *et al.* 1997; Friedrich *et al.* 2004). However, the fact that APACC needed about 0.2 s to recover from inactivation is inconsistent with the predominant involvement of L-type Ca^{2+} channels, as these require seconds to recover from inactivation in adult muscle (time constant between 1.1 s and 16 s depending on recovery voltage; Morrill *et al.* 1998, Harasztosi *et al.* 1998) or adult muscle fibres (> 5 s for charge movement recovery from inactivation, Collet *et al.* 2003). It is noteworthy that L-type gating, deactivation and tail current kinetics can be strongly modulated by auxiliary subunits (Andronache *et al.* 2007) and cAMP-dependent kinases (Johnson *et al.* 1997, 2005).

A fast current that passed through the L-type Ca^{2+} channel has been recorded following conditioning pulses only (Feldmeyer *et al.* 1990). This current failed to inactivate under voltage-clamp depolarization, which constitutes a major kinetic difference from the APACC described here. In the present study APACC was readily observed without a conditioning depolarization.

The description of the properties of the L-type Ca^{2+} channel above and the observation of the inactivation of APACC after a few action potentials at 10 Hz (Figs 4 and 5) are indeed inconsistent with any involvement of the L-type Ca^{2+} channel in conducting APACC. Therefore we can infer that APACC is conducted by a t-system protein other than the L-type Ca^{2+} channel. This protein must be present in the junctional membranes of the muscle fibre.

Physiological relevance

The contribution of APACC to the cytosolic Ca^{2+} transient associated with one action potential is small, but not negligibly small. Assuming a $[Ca^{2+}]_{t\text{-}sys}$ of 1.5 mM, the total APACC would contribute approximately 7 μM Ca^{2+} to the cytosol which corresponds to about 3% of the total Ca released from the SR (Posterino & Lamb, 2003). Directing this Ca^{2+} flux to the junctional region between the t-system and the SR, where the ryanodine receptors (RyRs) are located, we can speculate that the inhibitory effect exerted by Mg^{2+} ions on the activation sites on the RyRs would be reduced (Laver *et al.* 2004) and this would help prime the RyRs to open maximally more rapidly when the DHPRs are activated by the wave of depolarization associated with the action potential. Note that such a situation would only occur for the first action potential in a train of action potentials, because $[Ca^{2+}]$ in the junctional area will remain elevated following one action potential for the entire duration of the train of action potentials, and therefore additional action potential-activated Ca^{2+} fluxes would not be necessary. This provides a direct explanation as to why APACC should remain inactivated for the duration of trains of action potentials at frequencies above 10 Hz. If this inactivation mechanism becomes dysfunctional, then APACC may contribute to Ca^{2+} overload particularly in muscle disease states with disrupted Ca^{2+} homeostasis, like Duchenne muscular dystrophy.

Importantly, the APACC described in this paper may explain previous observations on twitch and tetanic responses in low Ca^{2+} bathing solutions when the Ca^{2+} flux is directed from the cytosol to the t-system lumen and $[Mg^{2+}]$ is high to maintain activatability of the voltage sensor (Melzer *et al.* 1995). Under such conditions, Ca^{2+} deprivation does not affect the membrane potential or the action potential and the magnitude of the single twitch response was markedly depressed, while the magnitude of the tetanic response was only slightly reduced (Lüttgau & Spiecker, 1979). Moreover, we show here that at $[Ca^{2+}]_{t\text{-}sys}$ below 0.1 mM, an action potential causes a rapid and brief outward flux of Ca^{2+} to the t-system (Figs 2 and 3). This reversal of APACC at low $[Ca^{2+}]_{t\text{-}sys}$ may act as a compensatory mechanism against Ca^{2+} loss from the t-system to ensure normal function of the voltage sensors.

The net influx of Ca^{2+} during an action potential also provides a mechanism to explain the increased uptake of

$^{45}Ca^{2+}$ during excitation, as shown in frog, rat and human skeletal muscle (Bianchi & Shanes, 1959; Curtis, 1966; Gissel & Clausen, 1999). It is particularly important to point out that the results published by Gissel & Clausen, 1999; Figs 2 and 4) indicate that the amount of Ca^{2+} entry per action potential in soleus muscle of the rat appears to decrease by factors of about 2, 3 and 4, as the frequency of stimulation increased from 0.5 Hz to 5, 10 and 20 Hz, respectively. This fully supports our observation that the APACC inactivates at higher rates of stimulation.

The Ca^{2+} entry from the t-system into the muscle fibre associated with APACC could also be used as a feedback mechanism to measure the level of muscle activity in fast-twitch muscles which are activated by short trains of action potentials eliciting tetani, with short periods of rest in between. With each APACC, the concentration of Ca^{2+} in the t-system decreases by some 0.25–0.5 mM (Fig. 4) and there is now growing evidence about the presence of molecules that can act as extracellular receptors triggering signals about changes in the extracellular $[Ca^{2+}]$ (Hofer, 2005) which can be used in various ways in the body.

With Ca^{2+} entering the skeletal muscle cell via APACC, what would be the role of SOCE that has been identified in muscle (Kurebayashi & Ogawa, 2001; Launikonis & Ríos, 2007) and how would these Ca^{2+} entry mechanisms work together to maintain normal $[Ca^{2+}]_{SR}$? It is clear that there is a threshold $[Ca^{2+}]_{SR}$ for SOCE activation in muscle (Launikonis & Ríos, 2007). Therefore, SOCE would become activated only if the $[Ca^{2+}]_{SR}$ was depleted below this level. However, in cases where $[Ca^{2+}]_{SR}$ does indeed fall to critically low levels, SOCE activation mobilizes a continuous Ca^{2+} inflow until $[Ca^{2+}]_{SR}$ has returned to a normal level (Launikonis & Ríos, 2007). Importantly SOCE is voltage independent, ensuring continuous Ca^{2+} inflow, as required regardless of the active state of the muscle. Thus the APACC complements SOCE to prevent severe $[Ca^{2+}]_{SR}$ depletion. A similar argument has been made for the complementary function of SOCE and ECCE in myotubes (Lyfenko & Dirksen, 2008).

In summary, we show for the first time that a Ca^{2+} flux is activated in the t-system of adult mammalian skeletal muscle by a single action potential. This flux appears to help with priming the RyRs to open maximally and more rapidly when the DHPRs are activated by an action potential. This flux is also inactivated by the increase in $[Ca^{2+}]$ on the cytoplasmic side of the tubular wall during repetitive stimulation, preventing potential Ca^{2+} overload. The flux described here provides an explanation for the observations of low frequency, excitation-induced uptake of Ca^{2+} in skeletal muscle (Bianchi & Shanes, 1959; Curtis, 1966; Gissel & Clausen, 1999) and potentially for changes in the action potential-induced force responses under conditions of Ca^{2+} deprivation (Lüttgau & Spiecker, 1979).

References

Allard B, Couchoux H, Pouvreau S & Jacquemond V (2006). Sarcoplasmic reticulum Ca^{2+} release and depletion fail to affect sarcolemmal ion channel activity in mouse skeletal muscle. *J Physiol* **575**, 68–81.

Andronache Z, Ursu D, Lehnert S, Freichel M, Flockeriz V & Melzer W (2007). The auxiliary subunit γ1 of the skeletal muscle L-type Ca^{2+} channel is an endogenous Ca^{2+} antagonist. *Proc Natl Acad Sci U S A* **104**, 17885–17890.

Bakker AJ, Head SI & Stephenson DG (1997). Time course of calcium transients derived from Fura-2 fluorescence measurements in single fast twitch fibres of adult mice and rat myotubes developing in primary culture. *Cell Calcium* **21**, 359–364.

Bannister RA, Pessah IN & Beam KG (2009). The skeletal L-type Ca^{2+} current is a major contributor to excitation-coupled Ca^{2+} entry. *J Gen Physiol* **133**, 79–91.

Baylor S & Hollingworth S (1988). Fura-2 calcium transients in frog skeletal muscle fibres. *J Physiol* **403**, 151–192.

Baylor S & Hollingworth S (2003). Sarcoplasmic reticulum calcium release compared in slow-twitch and fast-twitch fibres of mouse muscle. *J Physiol* **551**, 125–138.

Beam KG & Knudson CM (1988). Effect of postnatal development on calcium currents and slow charge movement in mammalian skeletal muscle. *J Gen Physiol* **91**, 799–815.

Berchtold MW, Brinkmeier H & Müntener M (2000). Calcium ion in skeletal muscle: its crucial role for muscle function, plasticity, and disease. *Physiol Rev* **80**, 1215–1265.

Berthier CA, Monteil A, Lory P & Strube C (2002). α1H mRNA in single skeletal muscle fibres accounts for T-type calcium current transient expression during fetal development in mice. *J Physiol* **539**, 681–691.

Bianchi CP & Shanes AM (1959). Calcium influx in skeletal muscle at rest, during activity, and during potassium contracture. *J Gen Physiol* **42**, 803–815.

Cairns SP, Buller SJ, Loiselle DS & Renaud JM (2003). Changes of action potentials and force at lowered $[Na^+]_o$ in mouse skeletal muscle: implications for fatigue. *Am J Physiol Cell Physiol* **285**, C1131–C1141.

Cherednichenko G, Hurne AM, Fessenden JD, Lee EH, Allen PD, Beam KG & Pessah IN (2004). Conformational activation of Ca^{2+} entry by depolarization of skeletal myotubes. *Proc Natl Acad Sci U S A* **101**, 15793–15798.

Cheung A, Dantzig JA, Hollingworth S, Baylor SM, Goldman YE, Mitchison TJ & Straight AF (2002). A small-molecule inhibitor of skeletal muscle myosin II. *Nat Cell Biol* **4**, 83–88.

Claflin DR, Morgan DL, Stephenson DG & Julian FJ (1994). The intracellular Ca^{2+} transient and tension in frog skeletal muscle fibres measured with high temporal resolution. *J Physiol* **475**, 319–325.

Collet C, Csernoch L & Jacquemond V (2003). Intramembrane charge movement and L-type calcium current in skeletal muscle fibers isolated from control and *mdx* mice. *Biophys J* **84**, 251–265.

Curtis BA (1966). Ca fluxes in single twitch muscle fibers. *J Gen Physiol* **50**, 255–267.

Delbono O & Stefani E (1993). Calcium transients in single mammalian skeletal muscle fibres. *J Physiol* **463**, 689–707.

DiFranco M, Capote J & Vergara JL (2005). Optical imaging and functional characterization of the transverse tubular system of mammalian muscle fibers using the potentiometric indicator di-8-ANEPPS. *J Membr Biol* **208**, 141–153.

Donaldson PL & Beam KG (1983). Calcium currents in fast-twitch skeletal muscle of the rat. *J Gen Physiol* **82**, 449–468.

Dutka TL, Murphy RM, Stephenson DG & Lamb GD (2008). Chloride conductance in the transverse tubular system of rat skeletal muscle fibres: importance in excitation–contraction coupling and fatigue. *J Physiol* **586**, 875–887.

Feldmeyer D, Melzer W, Pohl B & Zöllner P (1990). Fast gating kinetics of the slow Ca^{2+} current in cut skeletal muscle fibres of the frog. *J Physiol* **425**, 347–367.

Friedrich O, Both M, Gillis JM, Chamberlain JS & Fink RHA (2004). Mini-dystrophin restores L-type calcium currents in skeletal muscle of transgenic *mdx* mice. *J Physiol* **555**, 251–265.

Friedrich O, Ehmer T & Fink RHA (1999). Calcium currents during contraction and shortening in enzymatically isolated murine skeletal muscle fibres. *J Physiol* **517**, 757–770.

Fryer MW & Stephenson DG (1996). Total and sarcoplasmic reticulum calcium contents of skinned fibres from rat skeletal muscle. *J Physiol* **493**, 357–370.

Gissel H & Clausen T (1999). Excitation-induced Ca^{2+} uptake in rat skeletal muscle. *Am J Physiol Regul Integr Comp Physiol* **276**, R331–R339.

Gissel H & Clausen T (2000). Excitation-induced Ca^{2+} influx in rat soleus and EDL muscle: mechanisms and effects on cellular integrity. *Am J Physiol Regul Integr Comp Physiol* **279**, R917–R924.

Harasztosi CS, Sipos I, Kovacs L & Melzer W (1998). Kinetics of inactivation and restoration from inactivation of the L-type calcium current in human myotubes. *J Physiol* **516**, 129–138.

Hodgkin AL & Katz B (1949). The effect of sodium ions on the electrical activity of the giant axon of the squid. *J Physiol* **108**, 37–77.

Hofer AM (2005). Another dimension to calcium signaling. *J Cell Sci* **118**, 855–862.

Jacquemond V (1997). Indo-1 fluorescence signals elicited by membrane depolarization in enzymatically isolated mouse skeletal muscle fibers. *Biophys J* **73**, 920–928.

Johnson BD, Brousal JP, Peterson BZ, Gallombardo PA, Hockerman GH, Lai Y, Scheuer T & Catterall WA (1997). Modulation of the cloned skeletal muscle L-type Ca^{2+} channel by anchored cAMP-dependent protein kinase. *J Neurosci* **17**, 1243–1255.

Johnson BD, Scheuer T & Catterall WA (2005). Convergent regulation of skeletal muscle Ca^{2+} channels by dystrophin, the actin cytoskeleton, and cAMP dependent protein kinase. *Proc Natl Acad Sci U S A* **102**, 4191–4196.

Ju YK, Chu Y, Chaulet H, Lai D, Gervasio OL, Graham RM, Cannell MB & Allen DG (2007). Store-operated Ca^{2+} influx and expression of TRPC genes in mouse sinoatrial node. *Circ Res* **100**, 1605–1614.

Kurebayashi N & Ogawa Y (2001). Depletion of Ca^{2+} in the sarcoplasmic reticulum stimulates Ca^{2+} entry into mouse skeletal muscle fibres. *J Physiol* **533**, 185–199.

Lamb GD, Junankar P & Stephenson DG (1995). Raised intracellular $[Ca^{2+}]$ abolishes excitation–contraction coupling in skeletal muscle fibres of rat and toad. *J Physiol* **489**, 349–362.

Lamb GD & Stephenson DG (1994). Effects of intracellular pH and $[Mg^{2+}]$ on excitation-contraction coupling in skeletal muscle fibres of the rat. *J Physiol* **478**, 331–339.

Launikonis BS, Barnes M & Stephenson DG (2003). Identification of the coupling between skeletal muscle store-operated calcium entry and the inositol trisphosphate receptor. *Proc Natl Acad Sci U S A* **100**, 2941–2944.

Launikonis BS & Ríos E (2007). Store-operated Ca^{2+} entry during intracellular Ca^{2+} release in mammalian skeletal muscle. *J Physiol* **583**, 81–97.

Launikonis BS & Stephenson DG (2002). Properties of the vertebrate tubular system as a sealed compartment. *Cell Biol Int* **26**, 921–929.

Launikonis BS, Zhou J, Royer L, Shannon TR, Brum G & Ríos E (2005). Confocal imaging of $[Ca^{2+}]$ in cellular organelles by SEER, shifted excitation and emission ratioing. *J Physiol* **567**, 523–543.

Launikonis BS, Zhou J, Royer L, Shannon TR, Brum G & Ríos E (2006). Depletion "skraps" and dynamic buffering inside the cellular Ca^{2+} store. *Proc Natl Acad Sci U S A* **103**, 2982–2987.

Laver DR, O'Neill ER & Lamb GD (2004). Luminal Ca^{2+}-regulated Mg^{2+} inhibition of skeletal RyRs reconstituted as isolated channels or coupled clusters. *J Gen Physiol* **124**, 741–758.

Leung YM & Kwan CY (1999). Current perspectives in the pharmacological studies of store-operated Ca^{2+} entry blockers. *Jpn J Pharmacol* **81**, 253–258.

Lüttgau HC & Spiecker W (1979). The effects of calcium deprivation upon mechanical and electrophysiological parameters in skeletal muscle fibres of the frog. *J Physiol* **296**, 411–429.

Lyfenko AD & Dirksen RT (2008). Differential dependence of store-operated and excitation-coupled Ca^{2+} entry in skeletal muscle on STIM1 and Orai1. *J Physiol* **586**, 4815–4824.

Macdonald WA, Pedersen TH, Clausen T & Neilsen OB (2005). *N*-Benzyl-*p*-toluene sulphonamide allows the recording of trains of intracellular action potentials from nerve stimulated intact fast-twitch skeletal muscle of the rat. *Exp Physiol* **90**, 815–825.

Melzer W, Herrman-Frank A & Luttgau HC (1995). The role of Ca^{2+} ions in excitation-contraction coupling of skeletal muscle fibres. *Biochim Biophys Acta* **1241**, 59–116.

Morrill JA Jr, Brown RH & Cannon SC (1998). Gating of the L-type Ca channel in human skeletal myotubes: an activation defect caused by the hypokalemic periodic paralysis mutation R528H. *J Neurosci* **18**, 10320–10334.

Nielsen OB, Ørtenblad N, Lamb GD & Stephenson DG (2004). Excitability of the T-tubular system in rat skeletal muscle: roles of K^+ and Na^+ gradients and Na^+-K^+ pump activity. *J Physiol* **557**, 133–146.

Obukhov AG & Nowycky MC (2008). TRPC5 channels undergo changes in gating properties during the activation-deactivation cycle. *J Cell Physiol* **216**, 162–171.

Peachey LD (1966). The role of transverse tubules in excitation contraction coupling in striated muscles. *Ann N Y Acad Sci* **137**, 1025–1037.

Pedersen TH, de Paoli F & Nielsen OB (2005). Increased excitability of acidified skeletal muscle: role of chloride conductance. *J Gen Physiol* **125**, 237–246.

Posterino GS & Lamb GD (2003). Effect of sarcoplasmic reticulum Ca^{2+} content on action potential-induced Ca^{2+} release in rat skeletal muscle fibres. *J Physiol* **551**, 219–237.

Posterino GS, Lamb GD & Stephenson DG (2000). Twitch and tetanic force responses and longitudinal propagation of action potentials in skinned skeletal muscle fibres of the rat. *J Physiol* **527**, 131–137.

Royer L, Pouvreau S & Ríos E (2008). Evolution and modulation of intracellular calcium release during long-lasting, depleting depolarization in mouse muscle. *J Physiol* **586**, 4609–4629.

Sachetto R, Margreth A, Pelosi M & Carofoli E (1996). Colocalization of the dihydropyridine receptor, the plasma-membrane calcium ATPase isoform 1 and the sodium/calcium exchanger to the junctional-membrane domain of transverse tubules of rabbit skeletal muscle. *Eur J Biochem* **237**, 483–488.

Shimizu T, Janssens A, Voets T & Nilius B (2009). Regulation of the murine TRPP3 channel by voltage, pH, and changes in cell volume. *Pflügers Arch* **457**, 795–807.

Shirokova N, García J, Pizarro G & Ríos E (1996). Ca^{2+} release from the sarcoplasmic reticulum compared in amphibian and mammalian skeletal muscle. *J Gen Physiol* **107**, 1–18.

Shirokova N, García J & Ríos E (1998). Local calcium release in mammalian skeletal muscle. *J Physiol* **512**, 377–384.

Vandebrouck C, Martin D, Colson-Van Schoor M, Debaix H & Gailly P (2002). Involvement of TRPC in the abnormal calcium influx observed in dystrophic (*mdx*) mouse skeletal muscle fibers. *J Cell Biol* **158**, 1089–1096.

Westerblad H & Allen DG (1996). Intracellular calibration of the calcium indicator indo-1 in isolated fibers of *Xenopus* muscle. *Biophys J* **71**, 908–917.

Woods CE, Novo D, DiFranco M & Vergara JL (2004). The action potential-evoked sarcoplasmic reticulum calcium release is impaired in *mdx* mouse muscle fibres. *J Physiol* **557**, 59–75.

Zhou J, Yi J, Royer L, Launikonis BS, González A, García J & Ríos E (2006). A probable role of dihydropyridine receptors in repression of Ca^{2+} sparks demonstrated in cultured mammalian muscle. *Am J Physiol Cell Physiol* **290**, C539–C553.

Author contributions

All experiments were designed and performed at Rush University Medical Center, Chicago, by B.S.L. Data were analysed and interpreted by B.S.L., D.G.S. and O.F. The paper was written by B.S.L.

Acknowledgements

We thank Eduardo Ríos (Rush University Medical Center, Chicago) for comments on the manuscript. B.S.L. was a C. J. Martin Fellow of the National Health and Medical Research Council (NHMRC; Australia) and O.F. was an International Linkage Fellow of the Australian Research Council (ARC). This work was supported by an ARC Discovery Grant to B.S.L., and a NHMRC Project Grant to B.S.L. and D.G.S.